Supporting Information

Fluorescence-Enhanced BINOL-Hybridized Ladder-type Siloxanes and Their Sensing of Fe^{3+}

Keqian Zou,[1] Rongrong He,[1] Lizhong Zeng,[1] Yujia Liu,[2] Zheng Xu,[1] Masafumi Unno,[2] Liwen Xu[1] and Zhanjiang Zheng[1]

1. College of Material, Chemistry and Chemical Engineering, Key Laboratory of Organosilicon Chemistry and Material Technology, Ministry of Education, Zhejiang Key Laboratory of Organosilicon Material Technology, Hangzhou Normal University, Hangzhou, 311121, Zhejiang, P. R. China,

2. Department of Chemistry and Chemical Biology, Graduate School of Science and Technology, Gunma University, 1-5-1 Tenjin-cho, Kiryu 376-8515, Japan

Table of Contents

1. General information

THF and toluene were dried and distilled over metal sodium and benzophenone. Other reagents and solvents were used without further purification. Air and moisture-sensitive reactions were conducted under an argon atmosphere using standard Schlenk technique. Reactions were monitored by TLC using silica gel plates. Flash column chromatography was performed using silica (200-300 mesh). ^{1}H NMR, ^{13}C NMR, and ^{29}Si NMR spectra were acquired on a Bruker 400 MHz spectrometer in Acetone-d_6. Multiplicities were indicated as: s (singlet); d (doublet); t (triplet); q (quartet); or m (multiplet). High resolution mass spectra (HRMS) of the products were obtained using a Bruker Daltonics micro TOF-Q II spectrometer. Solvents used for spectroscopic measurements were of UV spectroscopic grade (Aldrich). UV absorption spectra were recorded on a LAMBDA750 UV-Vis spectrophotometer. Absolute quantum yields were measured on Hamamatsu Photonics C13534 UV-NIR Absolute PL Quantum Yield Measurement System. Fluorescence emission spectra were collected using a Hitachi F-7000 molecular fluorescence spectrometer (Hitachi, Japan) with 2.5-nm slit widths for both excitation (Ex) and emission (Em) wavelengths.

All calculations were performed using the Gaussian 16 suite of programs (Revision C.01).[1] Geometry optimizations were conducted without any symmetry constraints at the B3LYP/6-31G(d,p) level of theory. The shapes and energies of the frontier orbitals (HOMO and LUMO) were obtained at the same theoretical level, and the orbital plots were generated using GaussView 6.0.[2]

[1] M. J. Frisch, G. W. Trucks, H. B. Schlegel, et al.; Gaussian 16, Revision C.01; Gaussian, Inc.: Wallingford, CT, USA, 2016.

[2] A. D. Dennington, T. A. Keith, J. M. Millam; GaussView 6; Semichem, Inc.: Shawnee Mission, KS, USA, 2016.

2. Experimental procedures

Synthesis of ladder-type compound L1.

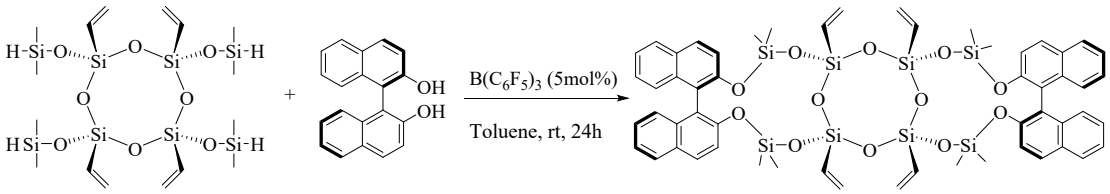

L1

To a 100 mL flask, (*R*)-binaphthol (1.15 g, 4 mmol, 2 eq.) and pentafluorophenyl borane (51.2 mg, 0.1 mmol, 5 mol%) were added. Freshly distilled toluene (30 mL) was then added and the reaction mixture was stirred at room temperature. Then, hydrosilyl-substituted all-cis-tetravinylcyclotetrasiloxane $[ViSi(OSiMe_2H)O]_4$ (1.17 g, 2 mmol, 1 eq.) diluted with toluene (10 mL) was added slowly. After addition, the mixture was stirred at room temperature for 24 hours. Then, 20 mL of water was added for quenching. The mixture was extracted with ethyl acetate and brine three times, dried over Na_2SO_4, and concentrated under reduced pressure. The crude product was purified by flash chromatography (PE/EA 300:1) to give **L1** as a white solid (0.8 g, 35% yield).

^{1}H NMR (400 MHz, Acetone-d_6) δ 7.97-7.88 (m, 8H), 7.38-7.20 (m, 12H), 7.07-7.04 (m, 4H), 6.1 (dd, J = 12.0 Hz and 4.4 Hz, 2H), 6.02-5.98 (m, 4H), 5.63-5.57 (m, 2H), 5.41-5.35 (m, 2H), 5.25-5.16(m, 2H), 0.31 (s, 6H), 0.23 (s, 6H), -0.18 (s, 6H), -0.22 (s, 6H).

^{13}C NMR (101 MHz, Acetone-d_6) δ 151.10, 136.47, 135.86, 135.26, 132.40, 131.25, 130.76, 130.62, 130.04, 129.92,128.98, 128.92, 127.03, 126.91, 126.27, 125.52, 124.67, 124.41, 123.74, 123.25, 122.24, 122.18, 121.86, 0.77, 0.30, 0.01, -0.06.

^{29}Si NMR (99 MHz, Acetone-d_6) δ -12.28, -12.62, -80.83, -81.23 ppm.

HRMS (ESI-TOF) m/z Calcd. for $C_{56}H_{60}O_{12}Si_8Na$ $[M+Na]^+$: 1171.2131; Found:1171.2125.

Synthesis of ladder-type compound L2.

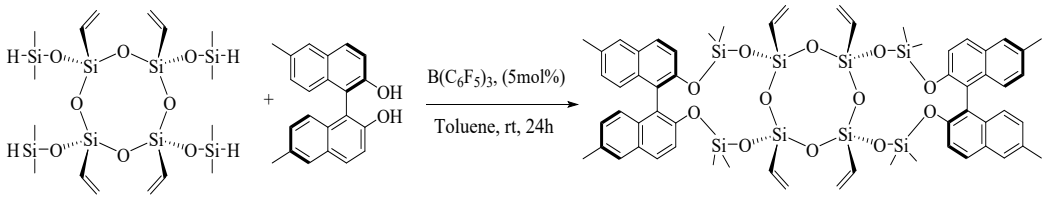

L2

To a 100 mL flask were added 6-methyl-(*R*)-binaphthol (1.26 g, 4 mmol, 2 eq.), pentafluorophenyl borane (51.2 mg, 0.1 mmol, 5mol%), and freshly distilled toluene (30 mL), the reaction mixture was stirred at room temperature. Then hydrosilyl-substituted all-*cis*-tetravinylcyclotetrasiloxane $[ViSi(OSiMe_2H)O]_4$ (1.17 g, 2 mmol, 1 eq.) diluted with toluene (10 ml) was added slowly. After addition, the mixture was stirred at room temperature for 24 hours. Then 20 ml of water was added for quenching, and the mixture was extracted with ethyl acetate and brine for 3 times,dried over Na_2SO_4 and concentratedunder reduced pressure. The crude product was purified by flash chromatography (PE/EA 300:1) to give **L2** in 10% yield (0.24 g), as a yellow solid.

^{1}H NMR (400 MHz, Acetone-d_6) δ 7.84(d, J = 8.8 Hz, 2H), 7.77 (d, J = 8.8 Hz, 2H), 7.67 (d, J = 7.6 Hz, 4H), 7.26 (d, J = 8.8 Hz, 2H), 7.07 (t, J = 7.2 Hz, 4H), 6.97-6.94 (m, 4H), 6.14 (dd, J = 12.8 Hz and 6.0 Hz, 2H), 6.02-5.98 (m, 4H), 5.62-5.58 (m, 2H), 5.43-5.36 (m, 2H), 5.26-5.18 (m, 2H), 2.42 (d, J = 2.8 Hz, 12H), 0.30 (s, 6H), 0.22 (s, 6H), -0.18 (s, 6H), -0.20 (s, 6H).

^{13}C NMR (101 MHz, Acetone-d_6) δ 150.64, 150.46, 136.40, 135.81, 133.91, 133.63, 133.48, 132.47, 131.36, 130.95, 130.81, 129.23, 129.15, 129.11, 129.04, 127.91, 127.83, 126.29, 123.26, 122.25, 122.16, 121.83, 32.40, 23.39, 21.46, 14.46, 0.76, 0.37, 0.04, 0.02.

^{29}Si NMR (99 MHz, Acetone-d_6) δ -12.89, -13.16, -80.96, -81.44 ppm.

HRMS (ESI-TOF) m/z Calcd. for $C_{60}H_{68}O_{12}Si_8Na$ $[M+Na]^+$: 1227.2757; Found:1227.2738.

3. Fluorescence spectra of compound **L1** in MeOH with the increasing concentration of Fe^{3+}

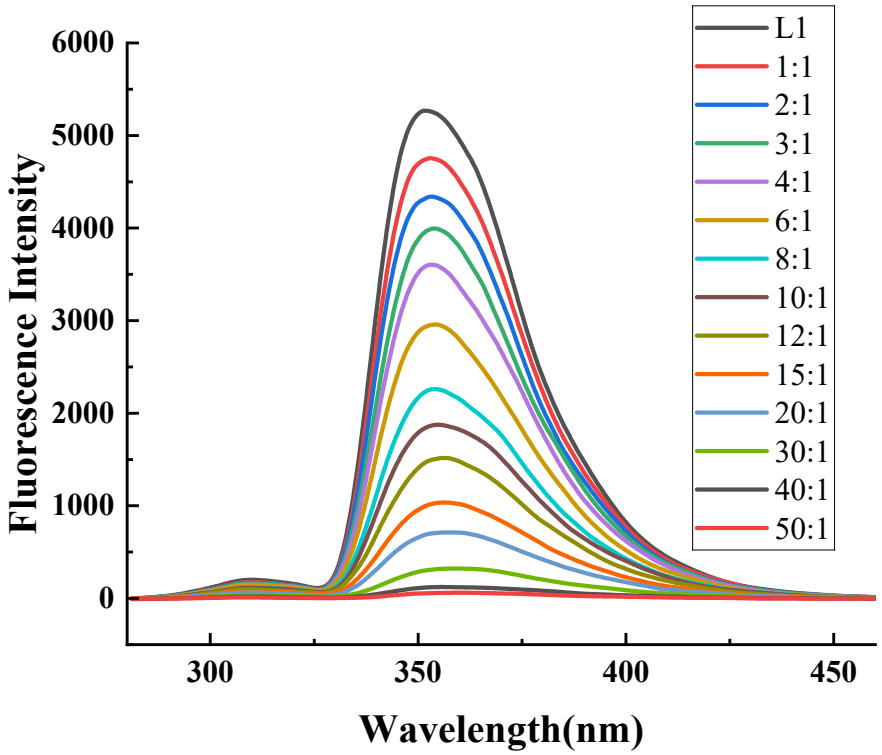

Figure S1 Changes in the emission spectra (λ_{ex}= 260 nm) of **L1** (10 μM) in MeOH upon the addition of increasing amounts of Fe^{3+}.

4. Fluorescence spectra of compound **L2** in MeOH with the increasing concentration of Fe^{3+}

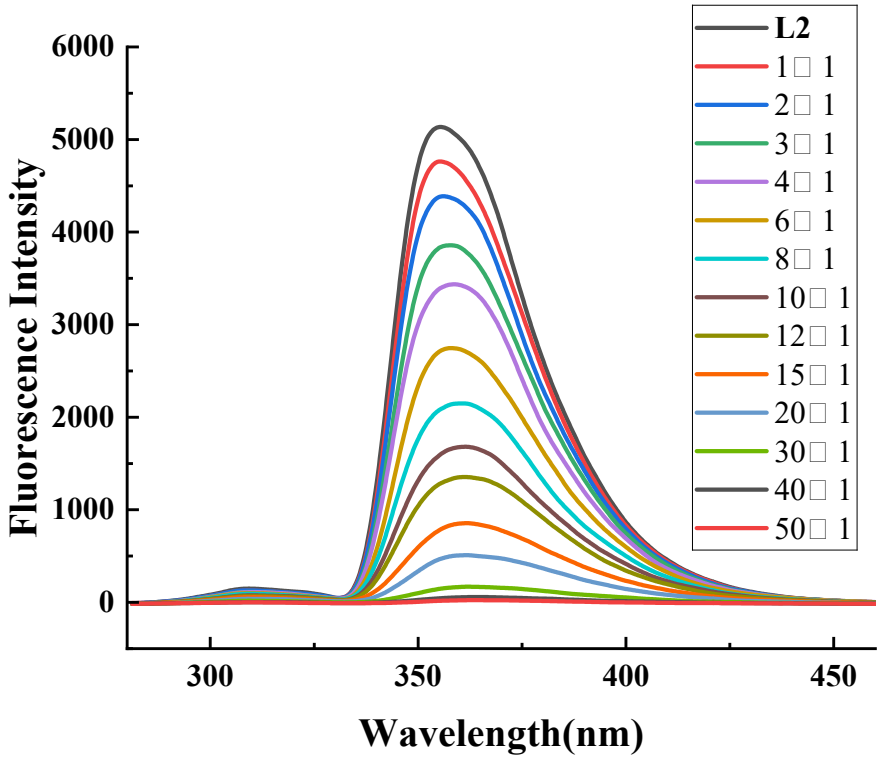

Figure S2. Changes in the emission spectra (λ_{ex}= 260 nm) of **L2** (10 μM) in MeOH upon the addition of increasing amounts of Fe^{3+}.

5. The Stern−Volmer plot for compounds **L1** and **L2**.

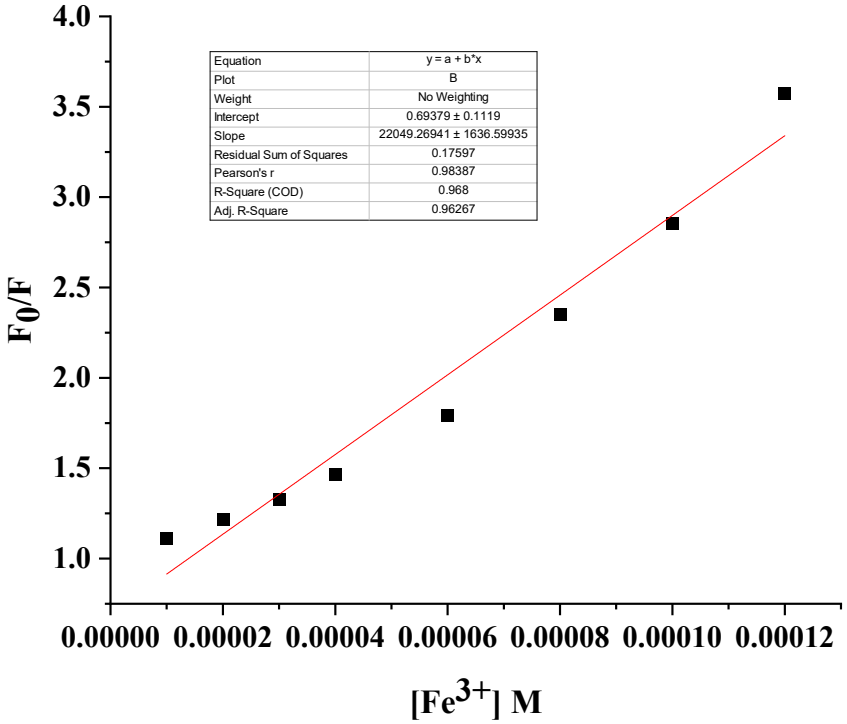

Figure S3. The Stern−Volmer plot at lower concentration of [Fe^{3+}] for compound **L1**.

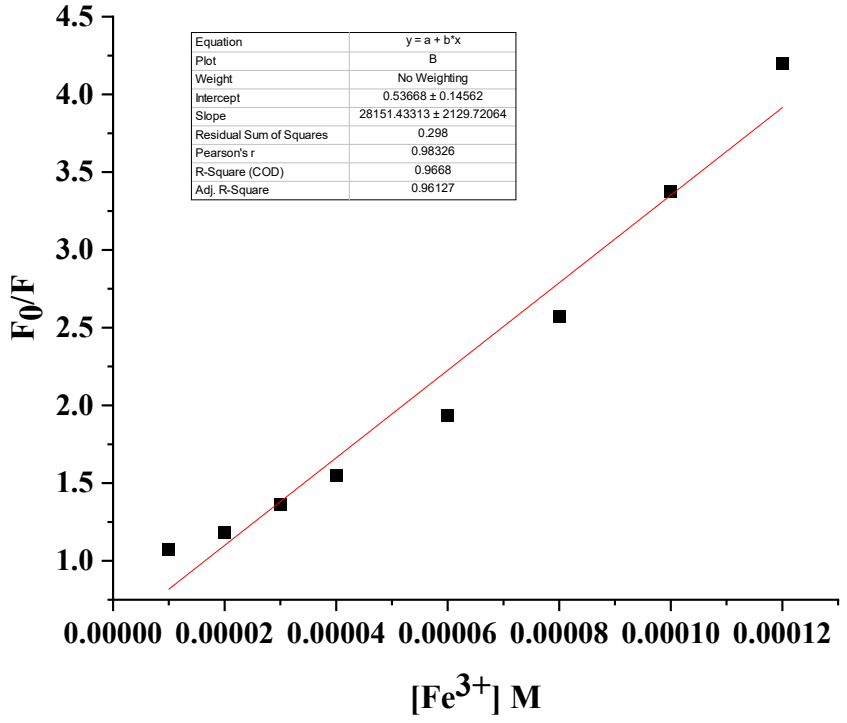

Figure S4. The Stern−Volmer plot at lower concentration of [Fe^{3+}] for compound **L2**.

6. The determination of the detecton limit for compounds **L1** and **L2**.

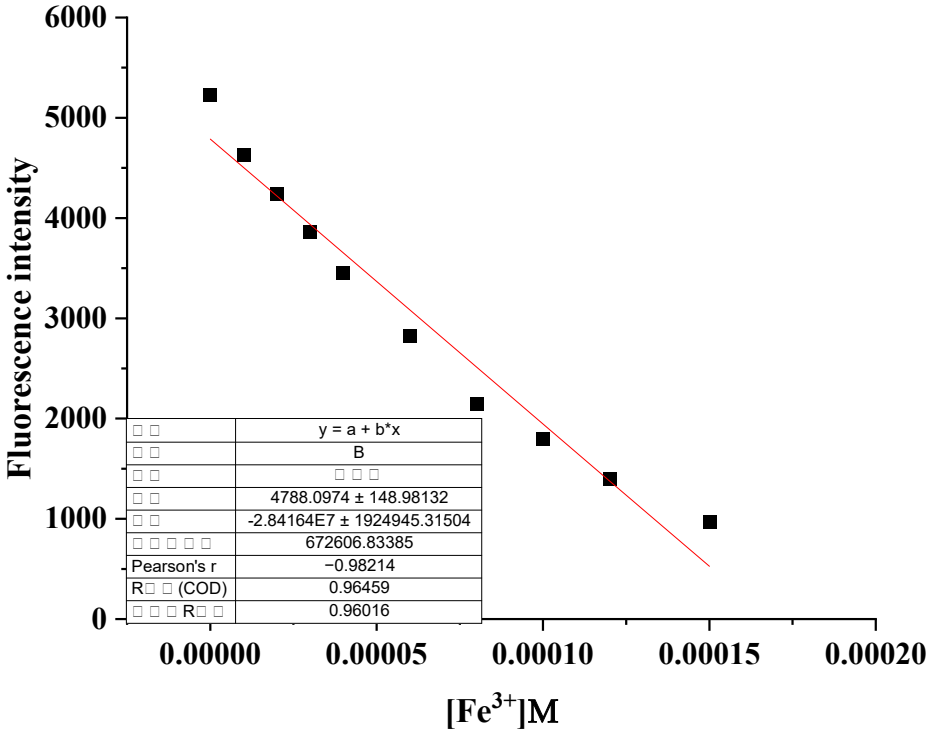

Figure S5. The linear fluorescence response for the titration of **L1** with Fe^{3+} to determine the detection limit (LOD). The LOD was calculated using the formula $3\sigma/k$, where σ = standard deviaition of blank (10 samples) and k = the slope of linear calibration curve.

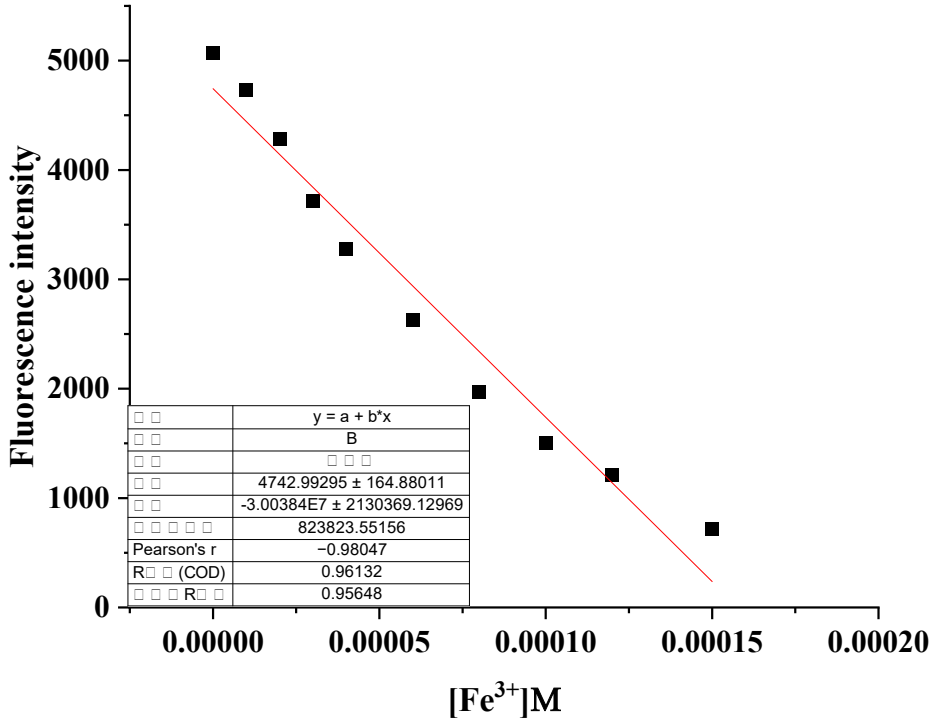

Figure S6. The linear fluorescence response for the titration of **L1** with Fe^{3+} to determine the detection limit (LOD). The LOD was calculated using the formula $3\sigma/k$, where σ = standard deviaition of blank (10 samples) and k = the slope of linear calibration curve.

7. Competitive sensing experiments of **L2** with various perchlorate salts of metal ions and Fe^{3+}.

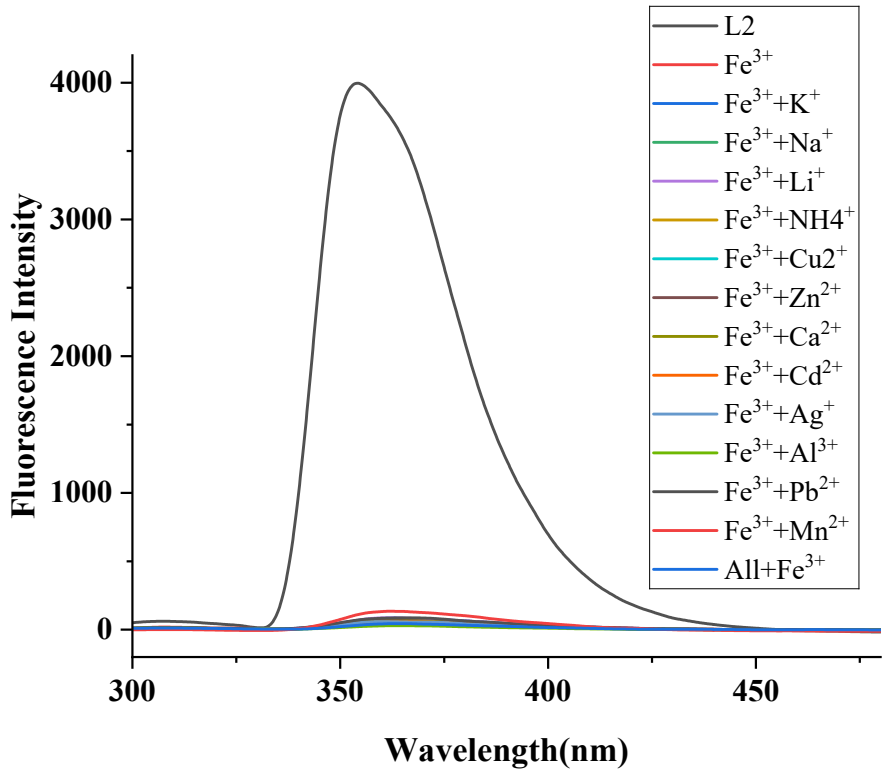

Figure S7. Fluorescent emission responses of **L2** (2.5 μM) with different perchlorate salts of metal ions (30 equiv) in the presence or absence of Fe^{3+} (30 equiv) in MeOH.

8. ESI-MS spectra of the mixture of compound **L1** and Fe^{3+} in Methanol.

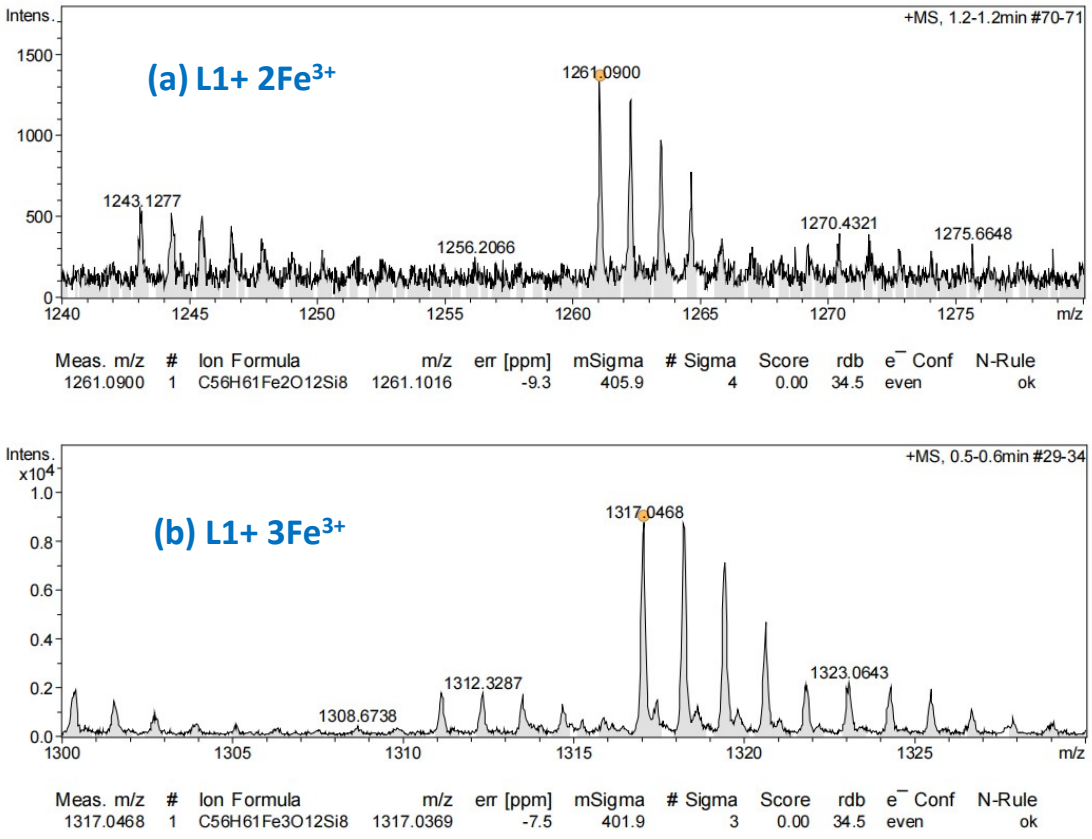

Figure S8. ESI-MS spectra of the mixture of compound **L1** and Fe^{3+} in Methanol.

9. HRMS-ESI spectra for compounds **L1** and **L2**.

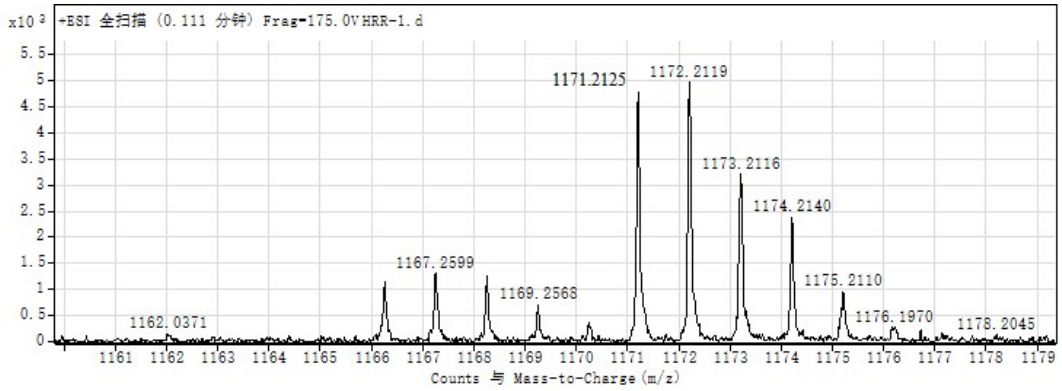

Figure S9. HRMS-ESI spectra for compounds **L1**

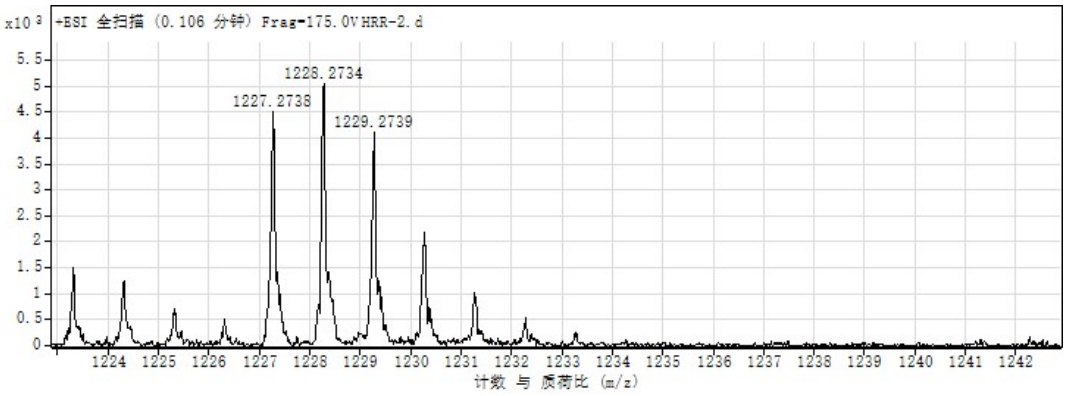

Figure S10. HRMS-ESI spectra for compounds **L2**

10. The fluorescence response of sensor **L1** and **L2** to Fe^{3+} at pH 4, 7, and 10.

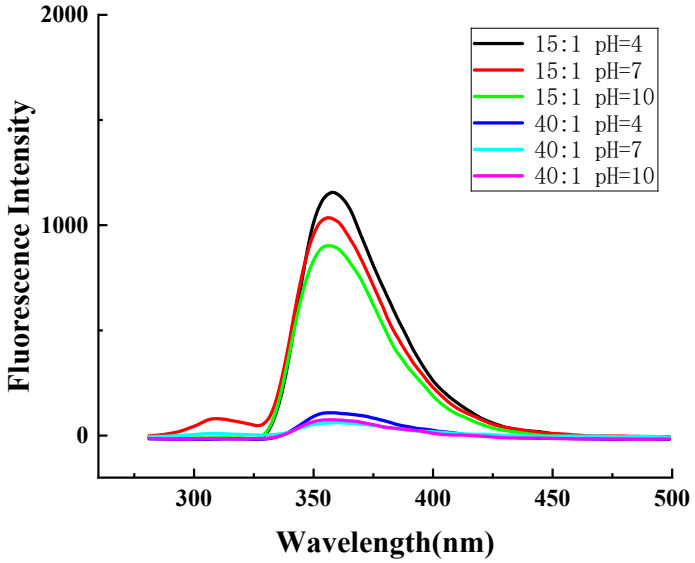

Figure S11. Fluorescent emission responses of **L1** (10 μM) in the presence of 15 or 40 equiv. of Fe^{3+} in MeOH/H_2O (125:1) at pH 4, 7 and 10.

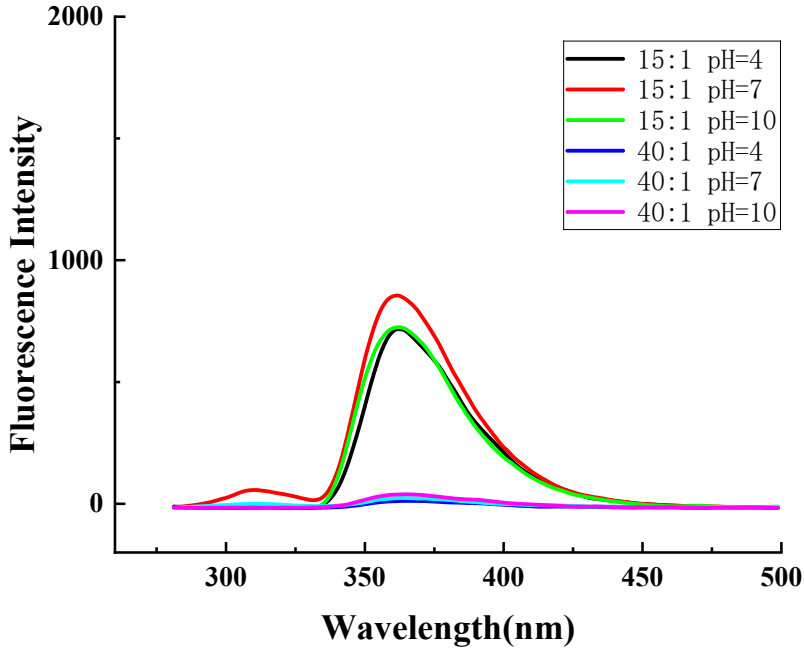

FigureS12. Fluorescent emission responses of **L1** (10 μM) in the presence of 15 or 40 equiv. of Fe^{3+} in MeOH/H_2O (125:1) at pH 4, 7 and 10.

11. NMR spectra for compounds Vi-TLS-BINOLs **L1** and **L2.**

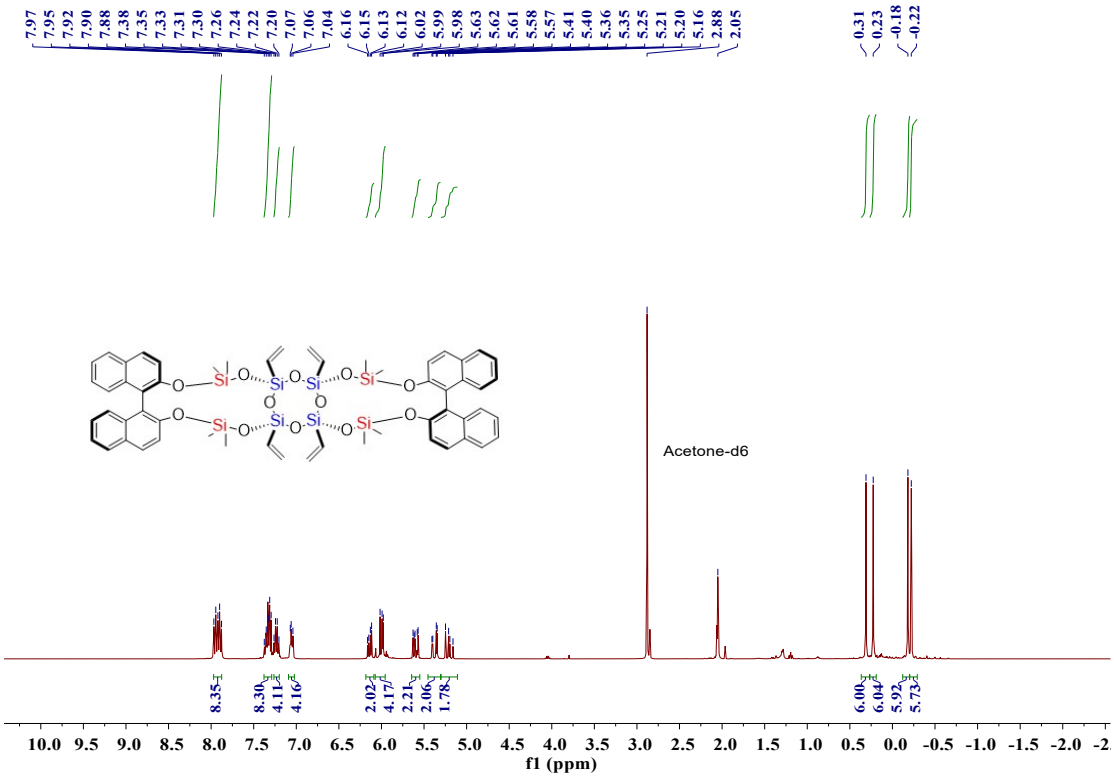

Figure S**13**. ^{1}H NMR spectrum of compound **L1**

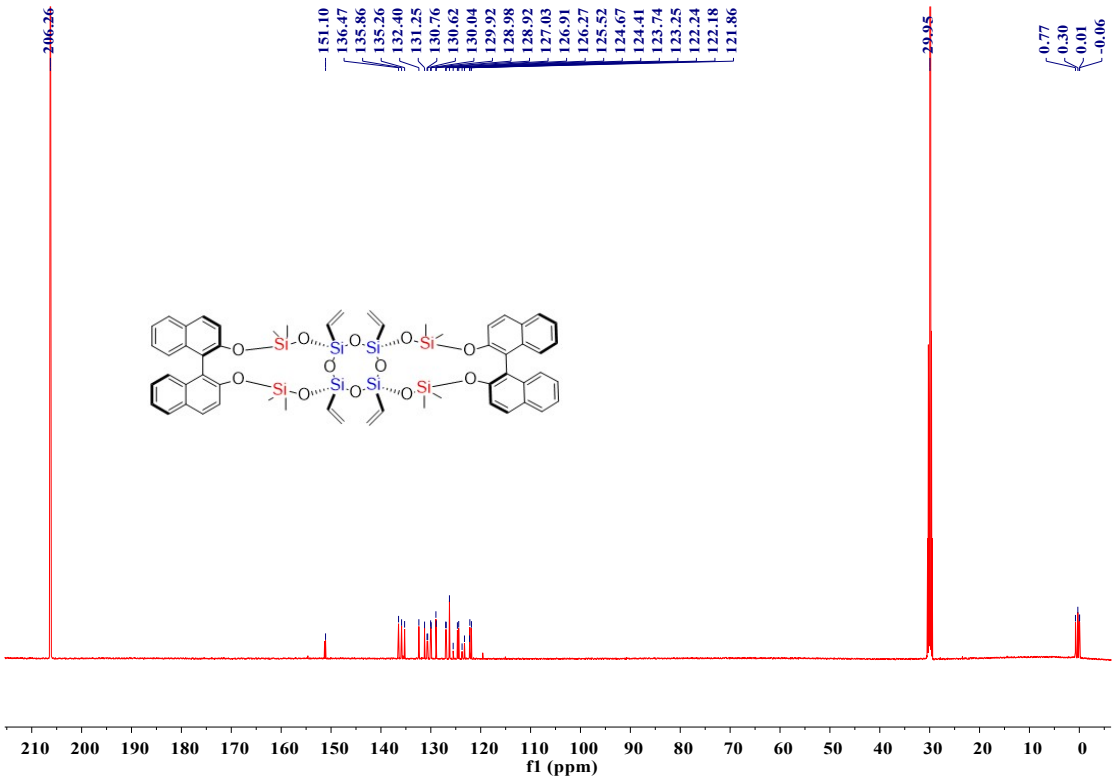

Figure S14. ^{13}C NMR spectrum of compound **L1**

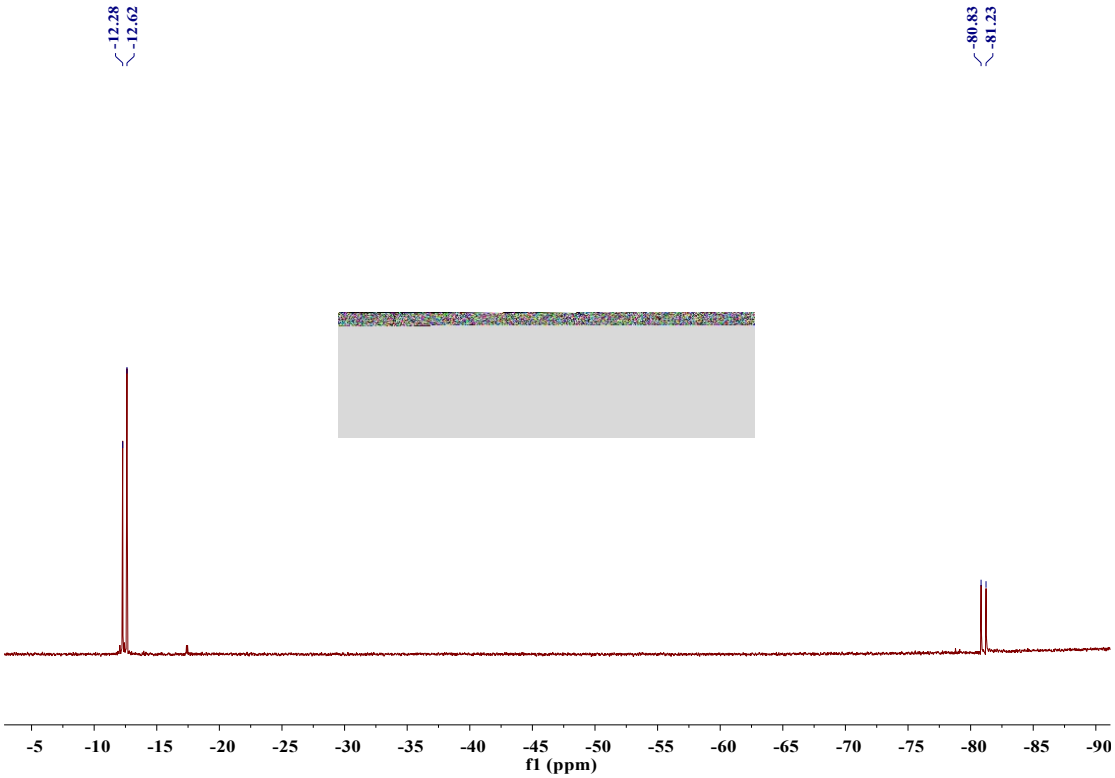

Figure S15. ^{29}Si NMR spectrum of compound **L1**

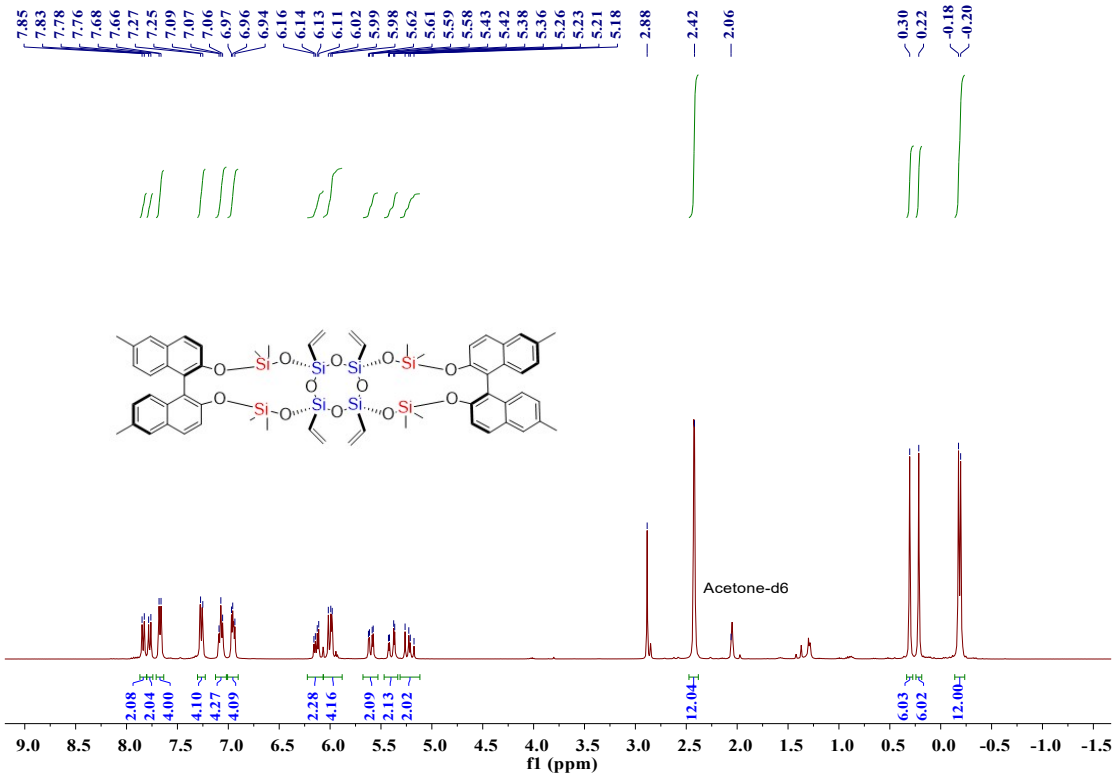

Figure S16. ^{1}H NMR spectrum of compound **L2**

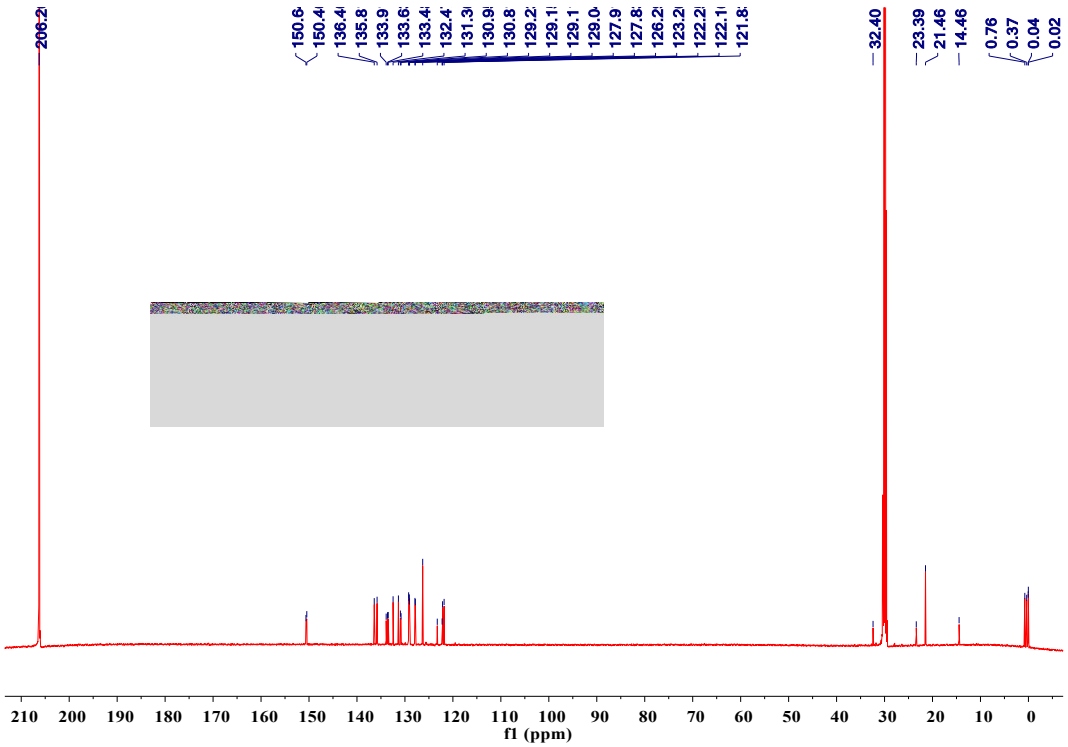

Figure S17. ^{13}C NMR spectrum of compound **L2**

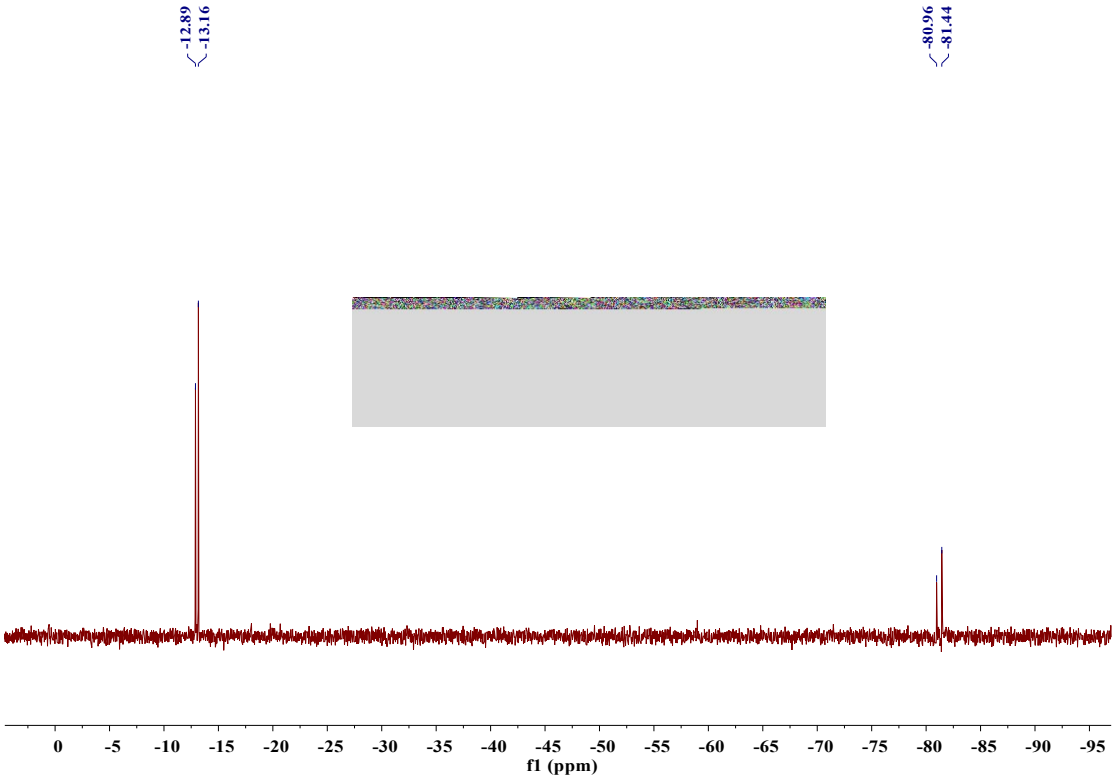

Figure S18. ^{29}Si NMR spectrum of compound **L2**

12. Recently reported Fe^{3+} chemosensors

Table S1 List of recently reported Fe^{3+} chemosensors

Sensor Material/Type	Sensing Mechanism	LOD	Sensing performance	Reference
Ru-Ni-BPY MOF	Static quenching	9.3 nM	Turn off	[1]
Gd−TCPP NCP	Coordination	98 nm	Turn off	[2]
N-CDs	IFE and static quenching	13.5 nm	Turn off	[3]
CDs	complexation	1.8 μM	Turn off	[4]
porous aromatic framework	Absorption competition quenching (ACQ)	38 μm	Turn off	[5]
CA-CDs	IFE and static quenching	0.96 μM	Turn off	[6]
$[Eu(Hpzbc)_2(NO_3)]\cdot H_2O$ (1-Eu)	interaction	26 μM	Turn off	[7]
Cl-CDs	IFE	0.36 μM	Turn off	[8]
glutathione protected gold nanoclusters	LMCT and complexation	227 nm	Ratiometric	[9]
Zn-MOF	FRET or PET	0.2 μM	Turn off	[10]
azopyrazole-b enzenesulfonamide derivative	Complexation	17 μM	Turn off	[11]
Coumarin-based probe	CHEF	1.28 μM	Turn on	[12]
M201P	Binding	0.51 μM	Turn off	[13]
W. coccinea CDs	Complexation	0.511 μM	Turn off	[14]
Cd-MOF	Electron-transfer transitions	79.6 μM	Turn off	[15]
bis-(naphthyl acetyl)-hydrazone (BNH)	Coordination	0.446 μM	Turn off	[16]
La-MOF	Binding	1.29 μM	Turn off	[17]

References:

1. J. Zhang, Z. Yin, W. Xiong, Q. Fan, F. Yu, F. Liao, et al., *Microchim. Acta*, 2025, **192**, 313.
2. X. Chen, Y. Wang, X. Zhao, B. Liu, Y. Xu and Y. Wang, *Microchim. Acta*, 2019, **186**, 63.
3. X. Zhou, G. Zhao, X. Tan, X. Qian, T. Zhang, J. Gui, et al., *Microchim. Acta*, 2019, **186**, 67.
4. M. Liu, Y. Xu, F. Niu, J. J. Gooding and J. Liu, *Analyst*, 2016, **141**, 2657-2664.
5. T.T. Ma, X. Zhao, Y. Matsuo, J. Song, R. Zhao, M. Faheem, M. Chen, Y.F. Zhang,

Y.Y. Tian, G.S. Zhu, *J. Mater. Chem. C*, 2019, **7**, 2327.

6. J. Shangguan, C. Qiao, Y. Zhang, N. Liu, T. Wei, Z. Chen, et al., *Nanoscale Adv*., 2025, **7**, 4161-4168.
7. G.-P. Li, G. Liu, Y.-Z. Li, L. Hou, Y.-Y. Wang and Z. Zhu, *Inorg. Chem*., 2016, **55**, 3952-3959.
8. Y. Wang, Y. Man, S. Li, S. Wu, X. Zhao, F. Xie, et al., *Spectrochim. Acta A Mol. Biomol. Spectrosc*., 2020, **226**, 117594.
9. S. Zhang, C. Zhang, X. Shao, R. Guan, Y. Hu, K. Zhang, et al., *RSC Adv.*, 2021, **11**, 17283-17290.
10. Y. D. Farahani and V. Safarifard, *J. Solid State Chem*., 2019, **275**,131-140.
11. A. Sayed, I. M. M. Othman, M. Hamam, H. Gomaa, M. I. Gadallah, M. A. Mostfa, et al., *J. Mol. Struct.*, 2021, **1225**, 129175.
12. S. Mahata, G. Janani, B. B. Mandal and V. Manivannan, *J. Photoch. Photobio. A*, 2021, **417**, 113340.
13. N. Kaewnok, N. Chailek, A. Petdum, K. Chanthana, C. Thummasoontorn, W. Panchan, et al., *J. Mol. Liq*., 2024, **403**, 124785.
14. J. Jose, R. Mohanraj, S. G.K, G. K.P and J. M. Jacob, *J. Fluoresc.* 2024, **35**, 3343-3353.
15. R.-M. Ma, M. Ray, Y.-G. Xia, J. Wang, S. Al-Sulaimi, M. Muddassir, et al., *Dyes Pigments*, 2024, **230**, 112316.
16. J. Liu, Y. Bao, Y. Chen, L. Wu, P.-Y. Chen and Q. Lin, *J. Lumin.*, 2024, **272**, 120624.
17. X. Si, J. Wang, C.-h. Xu, W. Zhang, C.-y. Shao and L.-r. Yang, *Colloids Surf. A*, 2024, **698**, 134517.